J|A|C|S
ARTICLES
Published on Web 12/05/2006

Stereospecificity in Metallocene Catalyzed Acrylate Polymerizations: The Chiral Orientation of the Growing Chain Selects Its Own Chain End Enantioface

Lucia Caporaso,[†] Josè Gracia-Budrìa,[†,‡] and Luigi Cavallo*,[†]

Contribution from the Dipartimento di Chimica, Università di Salerno, Via Salvador Allende, I-84081 Baronissi (SA), Italy, and Instituto de Biocomputación y Física de los Sistemas Complejos (BIFI), Edificio Cervantes, Corona de Aragón 42, 50009, Zaragoza, Spain.

Received August 7, 2006; E-mail: lcavallo@unisa.it

Abstract: The mechanism of stereocontrol in the site-controlled stereospecific polymerization of methyl methacrylate (MMA) with C_2- and C_S-symmetric zirconocenes is investigated with a DFT based approach. Our model explains the experimentally observed isospecificity in MMA polymerization with the C_2-symmetric *rac*-$C_2H_4(Ind)_2Zr$-based system as well as the experimentally observed syndiospecificity in MMA polymerization with the C_S-symmetric $Me_2C(Cp)(Flu)Zr$-based system. In both cases, the chiral metallocene induces a chiral orientation of the ester enolate growing chain. In turn, the chirally oriented growing chain selects its own enantioface. Comparison with the mechanism of stereocontrol operative in the case of propene polymerization by the same zirconocenes is performed to stress similarities and differences. Although analogies are expected, surprising differences also exist. The most peculiar is that the in the case of 1-olefins, the enantioselective event is selection between the enantiofaces of the prochiral monomer. Instead, in the case of acrylates, the enantioselective event is selection between the enantiofaces of the prochiral growing chain.

Introduction

Group 4 metallocenes are largely used for stereospecific 1-olefin polymerizations and the deep knowledge we have of the mechanism of stereocontrol indubitably contributed to the fast development of new catalysts with tailored properties.[1,2] The scope of metallocenes as polymerization catalysts is expanding to include the stereospecific polymerization of methyl methacrylate (MMA).[3−8] Using a C_2-symmetric zirconocene-based catalyst such as *rac*-$C_2H_4(Ind)_2ZrMe_2/B(C_6F_5)_3$, highly isotactic poly-MMA (PMMA), *%mmmm* pentads > 90%, is obtained at room temperature.[4,6] Very recently, quite stereoregular syndiotactic PMMA, *%rr* triads 64%, has been obtained at room temperature, using a C_S-symmetric zirconocene-based catalyst such as $[Me_2C(Cp)(Flu)Zr(THF)(OC(O^iPr)=CMe_2)]^+[MeB(C_6F_5)_3]^-$.[8]

Although the elementary steps of propene and MMA polymerization are clearly different, the extremely similar behavior (unsaturated monomer transformed into stereoregular polymers, see Scheme 1) might call for very similar mechanisms when the attention is focused on the transfer of chirality from the catalyst to the reactants.

Scheme 1

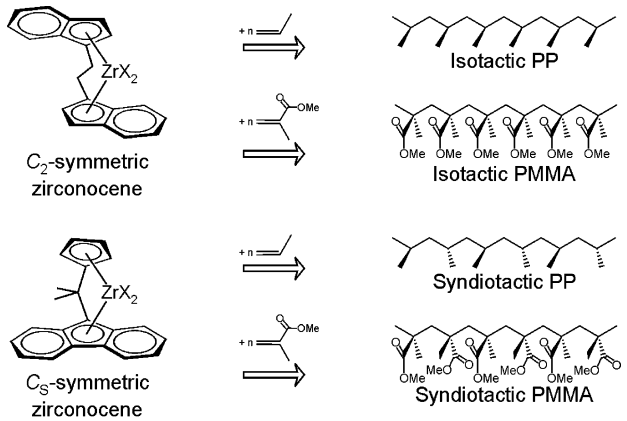

Of course, this is not the case. In fact, in site-controlled 1-olefin polymerizations the chirally oriented growing chain selects the enantioface of the incoming monomer.[9−12] Conversely, we herewith show that in the case of site-controlled MMA polymerization the chirally oriented growing chain does not select the monomer enantioface, but its own chain end enantioface.

[†] Università di Salerno.
[‡] BIFI.

(1) Coates, G. W. *Chem. Rev.* **2000**, *100*, 1223.
(2) Resconi, L.; Cavallo, L.; Fait, A.; Piemontesi, F. *Chem. Rev.* **2000**, *100*, 1253.
(3) Collins, S.; Ward, D. G.; Suddaby, K. H. *Macromolecules* **1994**, *27*, 7222.
(4) Soga, K.; Deng, H.; Yano, T.; Shiono, T. *Macromolecules* **1994**, *27*, 7938.
(5) Bolig, A. D.; Chen, E. Y. X. *J. Am. Chem. Soc.* **2004**, *126*, 4897.
(6) Cameron, P. A.; Gibson, V. C.; Graham, A. J. *Macromolecules* **2000**, *33*, 4329.
(7) Frauenrath, H.; Keul, H.; Hoecker, H. *Macromolecules* **2001**, *34*, 14.
(8) Rodriguez-Delgado, A.; Mariott, W. R.; Chen, E. Y.-X. *J. Organomet. Chem.* **2006**, *691*, 3490.
(9) Corradini, P.; Guerra, G.; Vacatello, M.; Villani, V. *Gazz. Chim. Ital.* **1988**, *118*, 173.
(10) Cavallo, L.; Guerra, G.; Vacatello, M.; Corradini, P. *Macromolecules* **1991**, *24*, 1784.
(11) Corradini, P.; Guerra, G.; Cavallo, L. *Acc. Chem. Res.* **2004**, *37*, 231.
(12) Corradini, P.; Guerra, G.; Cavallo, L. *Top. Stereochem.* **2003**, *24*, 1.

Scheme 2

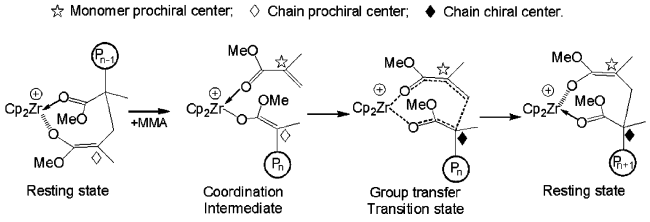

The mechanism of chain growth with monocomponent cationic zirconocene systems is a monometallic group transfer polymerization via an ester enolate intermediate[13,14] analogous to that proposed for MMA polymerization initiated by neutral lanthanocenes.[15,16] Experimental mechanistic studies evidenced that the resting state is the eight-membered ring of Scheme 2. The first step is displacement of the last ester unit from the electron-deficient Zr atom by a coordinating MMA molecule, whereas the second step is a relatively fast intramolecular Michael addition.[7,13,17,18] This mechanism is also supported by some theoretical studies.[14,19−21]

Broadly speaking, this mechanistic scenario is somewhat similar to what occurs in propene polymerization by zirconocenes. Also in that case the first step is displacement of a ligand (the counterion) from the Zr atom by a coordinating monomer molecule (propene), while the second step is a relatively fast chain growth step (propene enchainment through a Cossee-like transition state).

In both MMA and propene polymerization, the ligand displacement/monomer coordination step has been suggested to be the major contribution to the overall energy barrier.[22−24] However, in the case of the thoroughly investigated propene polymerization stereoselectivity and regioselectivity has been always rationalized at the moment of propene enchainment into the growing chain.[2,11,12,25−30] This mechanistic framework is also based on the experimental fact that in propene polymerization the activity of a given C_2-symmetric metallocene is highly dependent on the specific counterion used, whereas there is no detectable counterion effect on stereoselectivity and regioselectivity.[2,23,24,31−33] For this reason, to rationalize stereoselectivity in the case of site-controlled MMA polymerization, the main goal of the present work, we will focus on the transition state for the intramolecular Michael addition.

Although the elementary steps of Scheme 2 have been investigated in reasonable details, the mechanism of stereoselectivity is not completely clarified yet. Ziegler and co-workers have proposed a mechanism to explain the chain-end stereocontrol in the case of syndiospecific methyl acrylate polymerization with Cp_2Zr-based systems at low temperatures,[21] whereas Höcker and co-workers have postulated a mechanism to explain the isotacticity obtained in the polymerization of MMA with C_1-symmetric systems.[19]

Differently, in this work we present a mechanism to rationalize the isospecificity and the syndiospecificity in MMA polymerization by stereorigid C_2- and C_S-symmetric metallocenes, respectively. Comparison with the mechanism of stereocontrol operative in the case of propene polymerization by the same zirconocenes is also performed to stress similarities and differences. Although analogies are expected, surprising differences also exist. The most peculiar is that the in the case of 1-olefins, the enantioselective event is selection between the enantiofaces of the prochiral monomer. Instead, in the case of acrylates the enantioselective event is selection between the enantiofaces of the prochiral growing chain.

Computational Details

The Amsterdam Density Functional (ADF) program was used to obtain all the results discussed herein.[34,35] The electronic configuration of the molecular systems was described by a triple-ζ STO basis set on zirconium for 4s, 4p, 4d, 5s, 5p (ADF basis set TZV).[34] Double-ζ STO basis sets, augmented by one polarization function, were used for C and O (2s, 2p), and H (ADF basis sets DZVP).[34] The inner shells on zirconium (including 3d), carbon, and oxygen (1s) were treated within the frozen core approximation. Energies and geometries were evaluated using the local exchange-correlation potential by Vosko et al.,[36] augmented in a self-consistent manner with Becke's[37] exchange gradient correction and Perdew's[38,39] correlation gradient correction.

In the case of the C_{2V}-symmetric system, transition states were approached through a linear transit procedure starting from the coordination intermediates. The forming C−C bond was assumed as reaction coordinate during the linear transit scans. Full transition state searches were started from the maxima along the linear transit paths. In the case of the C_2- and C_S-symmetric systems, transition states were approached from the corresponding transition states found for the C_{2V}-symmetric system, by appropriate modification of the metallocene skeleton. These approximate transition states were first relaxed by keeping the forming C−C bond fixed. This partial geometry optimization was required to relax steric stress introduced by modification of the metallocene skeleton. Full transition state searches were started from the final geometries.

All geometries were localized in the gas phase. However, because MMA polymerization is usually performed in a rather polar solvent such as CH_2Cl_2, we performed single point energy calculations on the final geometries to take into account solvent effects. The ADF implementation of the conductor-like screening model (COSMO) was used.[40,41] A dielectric constant of 8.9 and a solvent radius of 2.94 Å were used to represent CH_2Cl_2 as the solvent. The following radii, in

(13) Li, Y.; Ward, D. G.; Reddy, S. S.; Collins, S. *Macromolecules* **1997**, *30*, 1875.
(14) Sustmann, R.; Sicking, W.; Bandermann, F.; Ferenz, M. *Macromolecules* **1999**, *32*, 4204.
(15) Yasuda, H.; Yamamoto, H.; Yokota, K.; Miyake, S.; Nakamuraf, A. *J. Am. Chem. Soc.* **1992**, *114*, 4908.
(16) Yasuda, H.; Yamamoto, H.; Yamashita, M.; Yokota, K.; Nakamura, A.; Miyake, S.; Kai, Y.; Kanehisa, N. *Macromolecules* **1993**, *26*, 7134.
(17) Rodriguez-Delgado, A.; Chen, E. Y. X. *Macromolecules* **2005**, *38*, 2587.
(18) Nguyen, H.; Jarvis, A. P.; Lesley, M. J. G.; Kelly, W. M.; Reddy, S. S.; Taylor, N. J.; Collins, S. *Macromolecules* **2000**, *33*, 1508.
(19) Hölscher, M.; Keul, H.; Höcker, H. *Chem.−Eur. J.* **2001**, *7*, 5419.
(20) Hölscher, M.; Keul, H.; Höcker, H. *Macromolecules* **2002**, *35*, 8194.
(21) Tomasi, S.; Weiss, H.; Ziegler, T. *Organometallics* **2006**, *25*, 3619.
(22) Vanka, K.; Xu, Z.; Ziegler, T. *Organometallics* **2004**, *23*, 2900.
(23) Bochmann, M. *J. Organomet. Chem.* **2004**, *689*, 3982.
(24) Rodriguez-Delgado, A.; Hannant, M. D.; Lancaster, S. J.; Bochmann, M. *Macromol. Chem. Phys.* **2004**, *205*, 334.
(25) Talarico, G.; Busico, V.; Cavallo, L. *J. Am. Chem. Soc.* **2003**, *125*, 7172.
(26) Milano, G.; Cavallo, L.; Guerra, G. *J. Am. Chem. Soc.* **2002**, *124*, 13368.
(27) Guerra, G.; Longo, P.; Corradini, P.; Cavallo, L. *J. Am. Chem. Soc.* **1999**, *121*, 8651.
(28) van der Leek, Y.; Angermund, K.; Reffke, M.; Kleinschmidt, R.; Goretzki, R.; Fink, G. *Chem.−Eur. J.* **1997**, *3*, 585.
(29) Rappé, A. K.; Skiff, W. M.; Casewit, C. J. *Chem. Rev.* **2000**, *100*, 1435.
(30) Yoshida, T.; Koga, N.; Morokuma, K. *Organometallics* **1996**, *15*, 766.
(31) Lancaster, S. J.; Walker, D. A.; Thornton-Pett, M.; Bochmann, M. *Chem. Commun.* **1999**, 1533.
(32) Hahn, S.; Fink, G. *Macromol. Chem. Phys.* **1997**, *18*, 117.
(33) Song, F.; Cannon, R. D.; Bochmann, M. *J. Am. Chem. Soc.* **2003**, *125*, 7641.
(34) 2.3.0, A., 1996.
(35) Baerends, E. J.; Ellis, D. E.; Ros, P. *Chem. Phys.* **1973**, *2*, 41.
(36) Vosko, S. H.; Wilk, L.; Nusair, M. *Can. J. Phys.* **1980**, *58*, 1200.
(37) Becke, A. D. *Phys. Rev. A* **1988**, *38*, 3098.
(38) Perdew, J. P. *Phys. Rev. B* **1986**, *33*, 8822.
(39) Perdew, J. P. *Phys. Rev. B* **1986**, *34*, 7406.
(40) Klamt, A.; Schüürmann, G. *J. Chem. Soc., Perkin Trans. 2* **1993**, 799.
(41) Pye, C. C.; Ziegler, T. *Theor. Chem. Acc.* **1999**, *101*, 396.

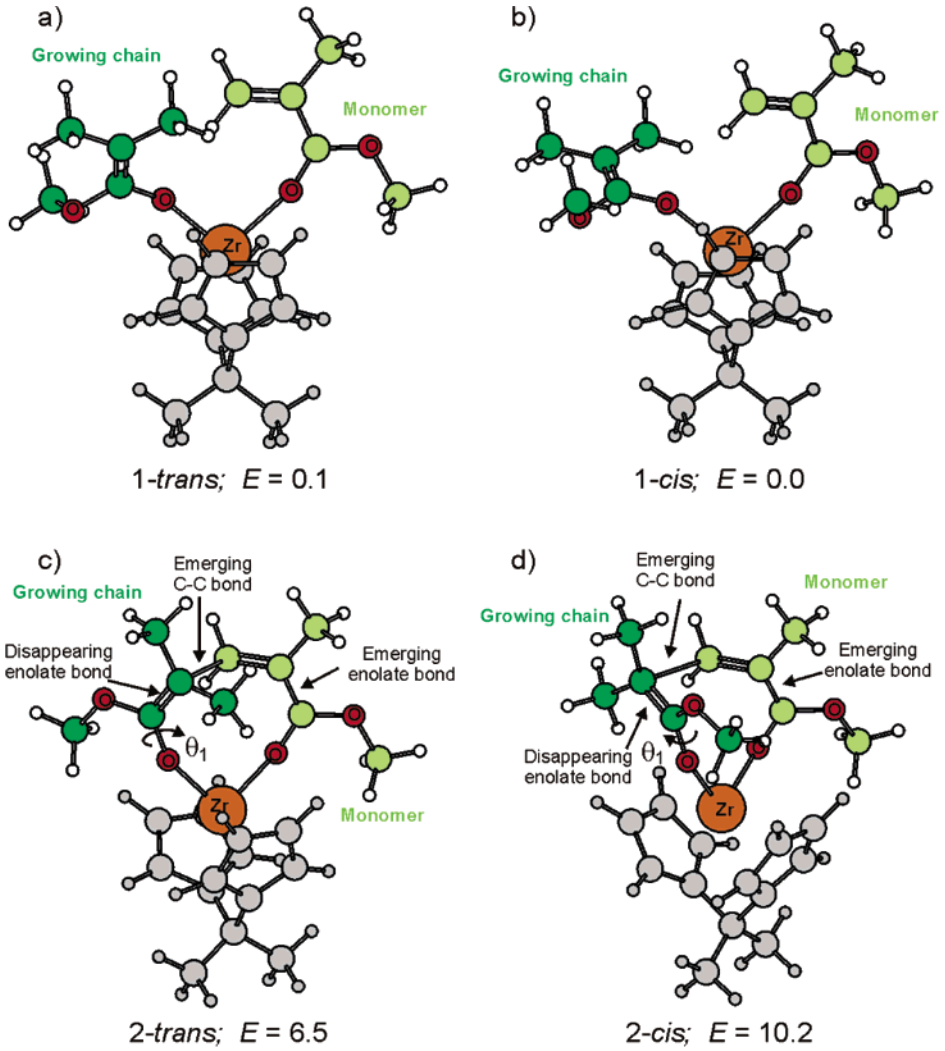

Figure 1. Structure of the coordination intermediates **1-*trans*** and **1-*cis***, and of the transition states **2-*trans*** and **2-*cis***, for the group transfer reaction in the presence of the $Me_2C(Cp)_2Zr$-based metallocene. Near to each structure is reported the energy, in kcal/mol, relative to the most stable coordination intermediate **1-*cis***.

Å, were used for the atoms: H 1.16, C 2.00, O 1.50, and Zr 2.40. All the reported energies include solvent effects.

Results and Discussion

Group Transfer Reaction with a C_{2v}-Symmetric Zirconocene. Although MMA polymerization by C_{2V}-symmetric metallocenes has been already investigated,[14,20,21] we briefly rediscuss it within our computational approach. This choice to underline some structural and energetic features that are of relevance for the mechanism of stereoselectivity with the C_2- and C_S-symmetric metallocenes discussed subsequently.

Coordination of MMA to the Zr atom leads to the coordination intermediates **1-*trans*** and **1-*cis*** of Figure 1. The two coordination intermediates are characterized by different relative orientation of the −OMe groups of MMA and of the ester enolate growing chain. In **1-*trans***, these −OMe groups are located on opposite sides of the metallocene equatorial belt, whereas in **1-*cis***, the two −OMe groups are on the same side. From the energetic viewpoint, **1-*trans*** and **1-*cis*** are of very similar energy, with **1-*cis*** less than 0.1 kcal/mol more stable than **1-*trans***. Starting from the **1-*trans*** and **1-*cis*** coordination intermediates, the transition states for the group transfer reaction, **2-*trans*** and **2-*cis*** of Figure 1, can be reached. As in the case of the coordination intermediates, the two transition states are characterized by different orientation of the −OMe groups of MMA and of the ester enolate growing chain. However, at the transition state, this geometric difference results in a substantial energy difference, with **2-*trans*** 3.7 kcal/mol more stable than **2-*cis***. The lower stability of the cis transition state can be associated to the almost eclipsed conformation, ∼−10°, assumed by the dihedral angle C═C−C═C around the emerging C−C bond in **2-*cis***. The calculated energy barrier for the group transfer reaction in CH_2Cl_2 is about 6.5 kcal/mol, which is close to the experimental activation energy for propagation in the case of MMA polymerization with the $Me_2C(Cp)(Ind)Zr$ based catalyst, 6.7 ± 0.5 kcal/mol.[7] Of course, such an agreement is fortuitous because the experimental activation energy is the result of the various steps that compose the reaction path of Scheme 2. Nevertheless, the fact that the calculated energy barrier is rather close to the experimental value validates our mechanistic approach.

As final remark, it is important to note that whereas the emerging C−C bond and its substituents are oriented away from the metal and from the metallocene skeleton both in **2-*cis*** and **2-*trans***, the two −OMe groups are oriented toward the metal

Scheme 3

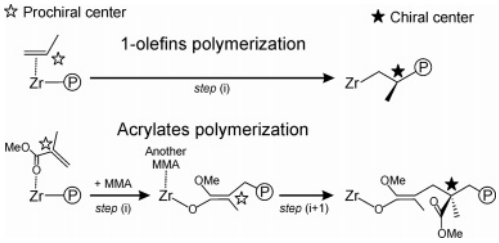

Scheme 4

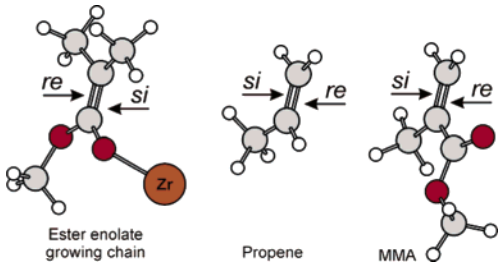

atom, i.e., they can easily suffer from steric interactions with the metallocene skeleton. Indeed, steric interactions between the −OMe groups and the metallocene skeleton will be key to rationalize enantioselectivity in the case of the C_2- and C_S-symmetric metallocenes.

Mechanism of Enantioselectivity: General Considerations. Before discussing the mechanism of enantioselectivity operative with C_2- and C_S-symmetric metallocenes, we underline some similarities and differences between the polymerization of MMA and propene.

First, it is fundamental to note that the MMA prochiral C atom that will be chiral in the final polymer (marked by an open star in the coordination intermediate of Scheme 2) still is sp^2 hybridized after it has been incorporated into the growing chain, see the resting state on the right of Scheme 2. In other words, after the new monomer has been enchained, its final chirality has not been determined yet. During the group transfer reaction prochirality is simply transferred from the monomer to the growing chain.

Differently, the prochiral C atom of the ester enolate growing chain (marked by an open diamond in the coordination intermediate of Scheme 2) is indeed converted into a chiral and sp^3 hybridized C atom (marked by a black diamond in the resting state of Scheme 2) during the group transfer reaction.

It is important to note that the mechanism herewith described is rather different from that operative in the case of 1-olefin polymerizations. In fact, in this case the chirality of the prochiral C atom of the monomer is determined when it is enchained, whereas in the case of acrylates it is determined one step later, see Scheme 3.

Because the C═C ester enolate bond of the growing chain is prochiral exactly in the same sense that the C═C double bond of propene or MMA is prochiral, see Scheme 4, we will refer to the two enantiofaces of the enolate bond of the growing chain as *re* and *si* enantiofaces, consistently with the nomenclature we adopted in the case of 1-olefin polymerizations.[11] Similarly, we label θ_1 the dihedral angle that defines the chiral orientation of the growing chain in space. In the case of MMA polymerization, the θ_1 angle is defined by the Zr−O(chain)−C(chain)−C(chain) bonds sequence, see Figure 1. This chiral orientation can be labeled as (−) or (+), depending on the sign assumed by θ_1.[11]

MMA Polymerization with a C_2-Symmetric Zirconocene. We move now to the transition states for the group transfer reaction in the presence of the C_2-symmetric *rac*-$Me_2C(Ind)_2$-Zr based system with a (*S*,*S*) coordinated bisindenyl ligand. In this case we had to consider four transition states. In fact, in the presence of the bisindenyl ligand both for the trans and cis transition states, two geometries, with a (+) and a (−) chiral orientation of the growing chain, are possible. The four transition states are reported in Figure 2. Calculations indicate that the (−)-*si*/trans transition state, which requires attack of the *si* enantioface of the growing chain, see Figure 2a, is favored. This energy preference is easily associated to reduced steric stress, because the −OMe groups of both the ester enolate growing chain and the MMA molecule are oriented away from the indenyl groups of the metallocene. Conversely, the (+)-*re*/trans transition state, which requires attack of the *re* enantioface of the growing chain, see Figure 2b, is 5.3 kcal/mol higher in energy due to steric interaction between both the −OMe groups and the bisindenyl ligand.[42]

In terms of steric interactions with the metallocene skeleton, both the (−)-*si*/cis and (+)-*re*/cis transition states are disfavored relative to the (−)-*si*/trans transition state by steric repulsion between the bisindenyl group and only one of the −OMe groups. However, they are of quite high energy relative to the favored (−)-*si*/trans transition state because calculations on the C_{2v}-metallocene indicated that a cis orientation of the growing chain and of the monomer is intrinsically less stable than a trans orientation. At the end, competition is between the (−)-*si*/trans and (+)-*re*/cis transition states, which results in a ΔE_{Stereo} of 5.3 kcal/mol.[43] This implies that the (*S*,*S*) coordinated ligand imposes a (−) chiral orientation to the growing chain that, in turn, selects the *si* enantioface of the growing chain.

Considering that in C_2-symmetric metallocenes the two coordination positions available to the ester enolate growing chain and to the monomer are homotopic,[12] for a metallocene with a (*S*,*S*) coordination of the ligand the (−)-*si*/trans transition state is favored at each insertion step. This rationalizes the formation of isotactic PMMA. The $\Delta E_{Stereo} = 5.3$ kcal/mol we calculated corresponds to > 99% of *mmmm* pentads at 25 °C, which is in reasonable agreement with the experimental value of > 90% obtained with C_2-symmetric metallocenes.[4,6]

MMA Polymerization with a C_S-Symmetric Zirconocene. We move now to the transition states for the group transfer reaction in the presence of the C_S-symmetric $Me_2C(Cp)(Flu)Zr$ based system with a *S* configuration at the chiral metal atom.[44] Analogously to the case of the C_2-symmetric system, we had to consider four transition states whose geometries are reported in Figure 3. Calculations indicate that the (−)-*si*/trans transition state is favored, see Figure 3a, although there are repulsive interactions between the −OMe group of the monomer and the

(42) A switch between the two enantiofaces of the growing chain only requires a rotation around the Zr−O(chain)−C(chain)−C(chain) dihedral angle. Of course, this is most likely to occur in the coordination intermediate, when the chain is attached to Zr with only one O atom.
(43) ΔE_{Stereo} is the energy difference between the lowest in energy transition states leading to opposite configurations of the chiral C atom in the polymer.
(44) Similarly to the case of propene polymerization by the same catalyst, the CIP nomenclature has been used to assign the absolute configuration to the metal atom. See ref 12.

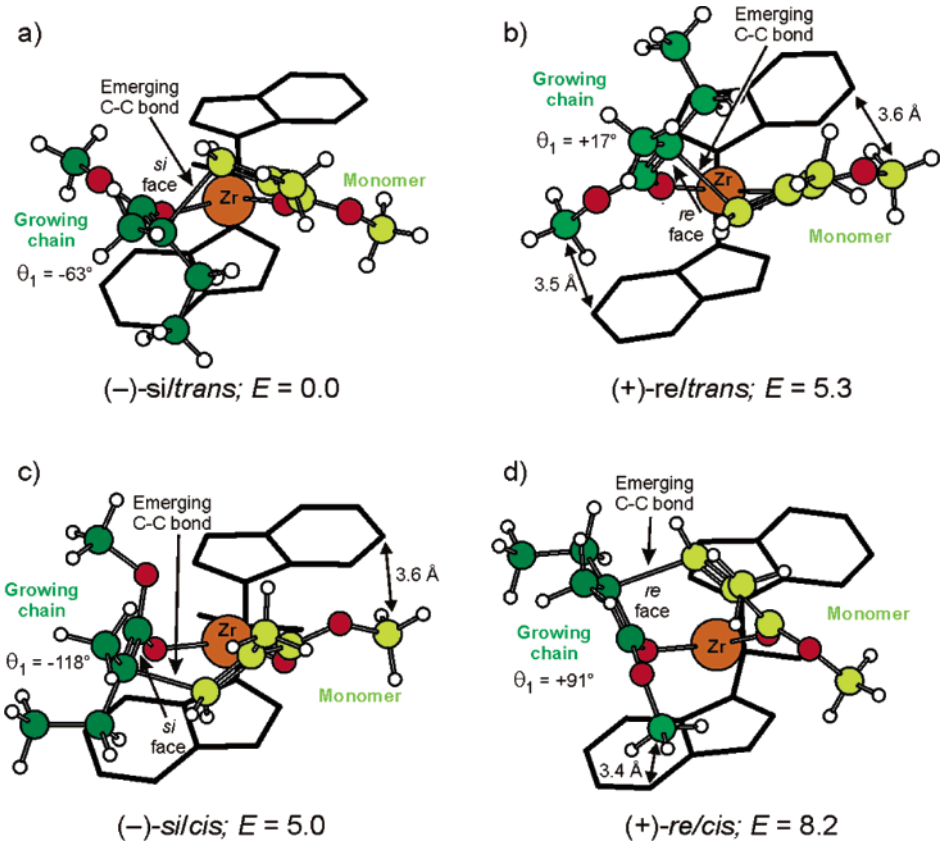

Figure 2. Transition states for the group transfer reaction with the C_2-symmetric *rac*-$Me_2C(Ind)_2Zr$ zirconocene containing a (*S*,*S*) coordinated bisindenyl ligand. Near to each structure is reported the energy, in kcal/mol, relative to the most stable transition state (−)-*si*/trans.

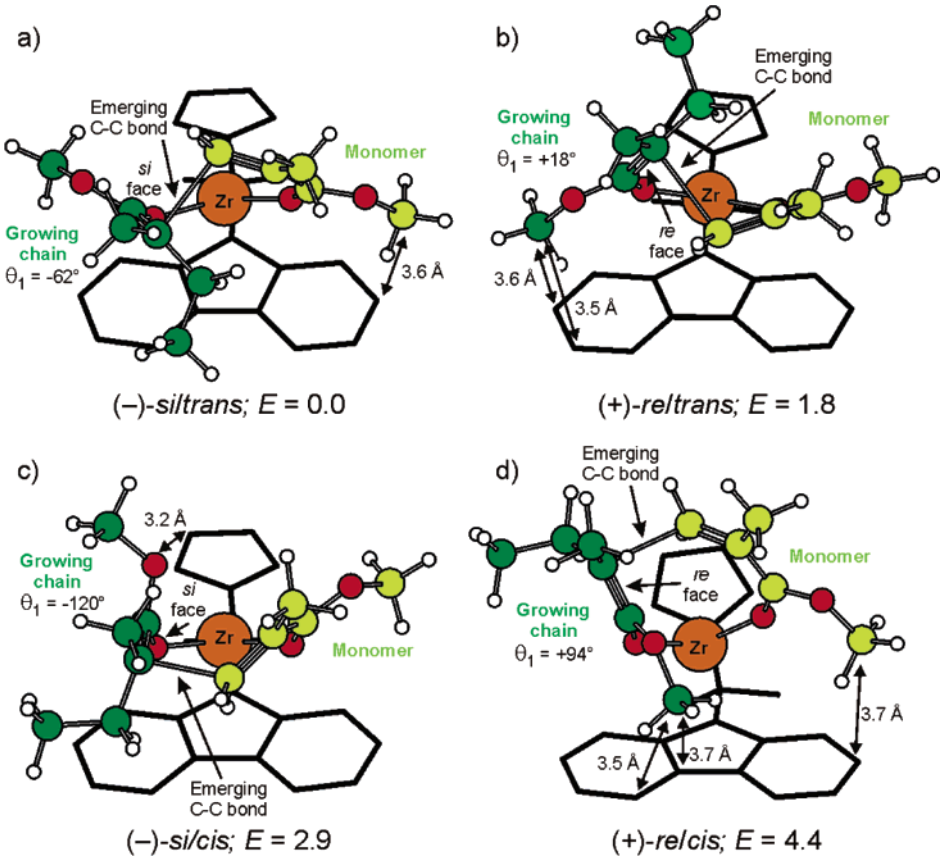

Figure 3. Transition states for the group transfer reaction with the C_S-symmetric $Me_2C(Cp)(Flu)Zr$ zirconocene with a *S* configuration at the Zr atom. Near to each structure is reported the energy, in kcal/mol, relative to the most stable transition state (−)-*si*/trans.

Flu ligand, as indicated by the short distances reported in Figure 3a. Also in this case, competition is with the (+)-*re*/trans transition state of Figure 3b, which is 1.8 kcal/mol higher in energy. This transition state is disfavored by repulsive interactions between the −OMe group of the growing chain and the Flu ligand, see the short distances reported in Figure 3b. The two cis transition states are both higher in energy, and it is likely they do not play any role.

Considering that in C_S-symmetric metallocenes the two coordination positions available to the ester enolate growing chain and to the monomer are enantiotopic,[12] in the framework of a regular chain migratory mechanism, the (−)-*si*/trans and the (+)-*re*/trans transition states are favored at subsequent insertion steps. This rationalizes the formation of syndiotactic PMMA. The $\Delta E_{Stereo} = 1.8$ kcal/mol we calculated corresponds to roughly 78% of *rr* triads at 25 °C, which is in reasonable agreement with the experimental value of 64%.[8]

The main difference between the C_S- and C_2-symmetric systems is that in the case of the C_2-symmetric system, one of the intrinsically favored trans transition states is able to place both the −OMe groups of the growing chain and of the monomer away from the bisindenyl ligand, whereas in the other trans transition state both the −OMe groups sterically interact with the bisindenyl ligand. Differently, in the case of the C_S-symmetric system, both trans transition states are destabilized by repulsive interaction between the −OMe group of the growing chain or of the monomer with the bulky Flu ligand. This results in lower ΔE_{Stereo} for the C_S-symmetric system relative to the C_2-symmetric system, and it is in qualitative agreement with the lower stereospecificity experimentally exhibited by C_S-symmetric systems. Of course, analogously to the case of propene polymerization, it is reasonable that alternative monomer approaches to the metal atom such as the "backside attack",[45,46] or site-isomerization reactions such as the "back-skip of the growing chain" contribute to lower the stereospecificity observed with C_S-symmetric catalysts.[46]

Conclusions

Although the mechanism of stereocontrol operative for acrylates might seem different from that operative for 1-olefins, in both cases stereocontrol originates from the chiral orientation of the growing chain, which is imposed by the chirality of the metallocene. However, in the case of 1-olefin polymerizations the chiral orientation of the growing chain selects between the two enantiofaces of the prochiral monomer, whereas in the case of acrylates the chiral orientation of the growing chain selects between the two enantiofaces of the prochiral growing chain.

The mechanism of stereocontrol presented here is unprecedented and, beside rationalizing a number of experimental data, it could be useful for the rational design of new strategies for the stereoselective polymerization of acrylates. We are currently extending this mechanism to explain the isospecificity of C_1-symmetric zirconocenes.

Acknowledgment. We acknowledge two of the reviewers for very useful comments. This work was supported by MIUR (Grant PRIN 2004) and by Basell Polyolefins. This publication is dedicated to the memory of Prof. Paolo Corradini.

Supporting Information Available: Cartesian coordinates and energies of all the structures. This material is available free of charge via the Internet at http://pubs.acs.org.

JA065703G

(45) Busico, V.; Cipullo, R.; Cutillo, F.; Vacatello, M.; Van Axel Castelli, V. *Macromolecules* **2003**, *36*, 4258.
(46) Chen, M.-C.; Roberts, J. A. S.; Marks, T. J. *J. Am. Chem. Soc.* **2004**, *126*, 4605.